



Al-pillared montmorillonite-based Mo catalysts: effect of the impregnation conditions on their structure and hydrotreating activity

P. Salerno*, S. Mendioroz, A. López Agudo

Instituto de Catálisis y Petroleoquímica, CSIC, Camino de Valdelatas s/n, Cantoblanco, Campus UAM, 29049 Madrid, Spain

Received 22 July 2002; accepted 15 April 2003

Abstract

The effects of the pH and medium of the impregnation solution on the surface structure and activity for gas oil hydrodesulfurization (HDS) of molybdenum catalysts supported on an Al-pillared montmorillonite have been studied. Catalysts were characterized by using X-ray diffraction, nitrogen and ammonia sorption measurements, temperature-programmed reduction, Raman spectroscopy, and X-ray photoelectron spectroscopy. It was found that impregnation at basic pH leads to the incorporation of molybdenum mainly in form of monomeric and polymeric species, with a substantial part of Mo species in the interlayer space of the Al-pillared clay, probably in interaction with the alumina pillars. Whereas, formation of small particles of bulk MoO₃ deposited on the external surface of the Al-pillared clay was favoured by impregnation at acid pH. The impregnation at pH 8.5 in a H₂O₂ solution produced abundant formation of incipient MoO₃ crystallites relatively well dispersed, partially located inside the porous system. The catalysts prepared at basic pH values had slightly higher HDS activity than those prepared at acid pH values.

© 2003 Elsevier B.V. All rights reserved.

Keywords: Aluminium-pillared clays; Montmorillonite; Sulfide molybdenum catalysts; Gas oil hydrodesulfurization

1. Introduction

Pillared clay minerals (PILCs) have been extensively synthesized and characterized over the past two decades and evaluated as catalysts in a wide range of reactions, mainly in acid catalysis (Pinnavaia, 1983; Burch, 1987; Figueras, 1988; Lambert and Poncelet, 1997). The application of new methods in PILCs synthesis and further improvements in their properties,

especially in hydrothermal stability and enhanced acidity, as well as the incorporation of transition metal ions into the pillars or on the pillared clay surface, have extended the possible use of these materials to other catalytic reactions, including those related to oil refining hydrotreating processes (Vaccari, 1999; Gil et al., 2000).

Referring to the applications of PILCs to the later reactions, we can refer to the early work on demetalization of heavy crude oil on Fe sulfide-pillared montmorillonite (Burch and Warburton, 1987); and more recently, the HDS of thiophene and consecutive hydrogenation of butene on chromia- and chromium

* Corresponding author. Fax: +34-91-585-4760.

E-mail address: patty@icp.csic.es (P. Salerno).

sulfide-pillared montmorillonite (Sychev et al., 1997). On the use of PILCs as support of the conventional metal sulfide catalysts, only a few studies have been reported and most of them using Al- or Al-metal-pillared clays. For example, different Al-pillared montmorillonites loaded with Ni were prepared and tested in thiophene HDS (Kloproge et al., 1993) and benzene hydrogenation (Louloudi and Papayannakos, 2000). The effect of Mo loading in the structure and HDS activity of MoS₂ supported on Ga-Al-pillared clay was reported by Pacheco et al. (1998). In the field of upgrading of fuel oil, mention should be made of using Al- and Ti-pillared clays (Ramos-Galvan et al., 1997), mixed Al-pillared clay-alumina extrudates (Monnier et al., 1993) and palygorskite-montmorillonite clays (Lur'e et al., 2000) as supports of Ni–Mo catalysts and their catalytic properties for hydrotreating of different fuel oil feedstocks. No particular attention has been paid to the influence of the method of incorporating molybdenum to PILC supports in relation with hydrotreating catalysts. However, it is widely known that the nature and distribution of Mo species incorporated to any support is strongly dependent on the preparation conditions (impregnation procedure, metal loading, solution pH, calcination conditions, etc.) and on the characteristics of the support (Topsøe et al., 1996). In the case of Al-pillared clays, as Mo species can be deposited on the silicic or aluminic part of these materials, the preparation conditions, particularly the impregnating pH, may have a profound influence on the nature and dispersion of the Mo species and, consequently, on catalytic activity.

The aim of this work was to study the effects that the pH and medium of the impregnation solution have on the structure of Mo catalysts supported on Al-pillared clays and their catalytic properties in gas oil hydrodesulfurization (HDS) and pyridine hydrogenation (HDN). This fundamental study will allow us to define the most appropriate conditions to support molybdenum on PILCs and then to apply the development of bimetallic hydrotreating catalysts. An additional objective of the present work was to take profit of recent advances in PILCs synthesis. For example, by using concentrated clay suspensions and pillaring solutions instead of conventional diluted solutions in order to produce large quantities of materials with the same surface properties (Storaro et al., 1996; Moreno

et al., 1997; Sanchez and Montes, 1998; Salerno et al., 2001).

2. Experimental

2.1. Preparation of the Al-PILC support and Mo catalysts

The starting material for the Al-pillared clay used as support of the catalysts was a montmorillonite from La Serrata de Nijar, Spain. This clay is a dioctahedral, high purity and iron-rich montmorillonite, with Ca, Mg and Na as the main exchangeable cations. Its structural formula, calculated from chemical analysis and cation exchange capacity measurements ($\text{CEC} = 1.19 \text{ meq g}^{-1}$), was $\text{X}_{0.66}(\text{Si}_8)^{\text{IV}}(\text{Al}_{2.78}\text{Fe}_{0.68}\text{Mg}_{0.58}\text{Mn}_{0.08})^{\text{VI}}\text{O}_{20}(\text{OH})_4$; specific surface area (S_{BET}), $81 \text{ m}^2 \text{ g}^{-1}$; micropore volume (V_{μ}), $0.013 \text{ cm}^3 \text{ g}^{-1}$; total pore volume (V_t), $0.744 \text{ cm}^3 \text{ g}^{-1}$; and acidity, measured by NH₃ adsorption at room temperature, $0.8 \text{ meq NH}_3 \text{ g}^{-1}$.

The pillaring reaction of the clay was carried out using a highly concentrated clay suspension procedure (Salerno et al., 2001) similar to that described by Storaro et al. (1996). The pillaring agent was a 50% aqueous solution of Locron[®], an Al₁₃ Keggin cation supplied by Hoechst. This solution was added dropwise to a 50 wt.% suspension of the natural clay, as received, in acetone under stirring for 1 h. The amount of aluminium used was 30 meq Al g^{-1} clay. The final suspension, after decantation, was washed by dialysis with distilled water until free of ions, dried in static air atmosphere at 353 K and finally calcined at 773 K for 2 h. The resulting pillared material (designated as Loc) had a basal spacing $d_{001} = 1.8 \text{ nm}$ and its textural properties are summarized in Table 1.

Several molybdenum catalysts (10.71 wt.% MoO₃) were prepared by incipient wetness impregnation of the Al-pillared clay support with a solution of (NH₄)₆Mo₇O₂₄x4H₂O (AHM) in different media and pHs, as shown in Table 1. After impregnation, the samples were dried in static air at room temperature for 24 h and then calcined at 673 K for 4 h. The catalysts were denoted by Mo(x)/Loc, being x the pH of the impregnating solution. For comparative purposes, a sample of 10.7 wt.% MoO₃ supported on the starting clay was prepared at incipient wetness impregnation and pH 10.

Table 1
Preparation conditions, textural properties and nomenclature of Mo(x)/Loc catalysts

Catalyst	Impregnation pH and medium	S_{BET} ($\text{m}^2 \text{g}^{-1}$)	V_{μ} ($\text{cm}^3 \text{g}^{-1}$)	V_{t} ($\text{cm}^3 \text{g}^{-1}$)	Total acidity ($\text{meq NH}_3 \text{g}^{-1}$)
Clay	–	81	0.013	0.744	0.8 ± 0.1
Loc	–	320	0.090	0.940	2.0 ± 0.2
Mo(10)/Loc	10; NH_4OH solution	202	0.061	0.149	2.5 ± 0.3
Mo(8.5)/Loc	8.5; H_2O_2 solution	214	0.065	0.155	2.0 ± 0.2
Mo(6.5)/Loc	6.5; H_2O solution	237	0.072	0.177	2.5 ± 0.3
Mo(4)/Loc	4; citric acid solution	239	0.070	0.180	2.0 ± 0.2

V_{μ} and V_{t} are the micro and total porous volume, respectively.

2.2. Characterization techniques

Powder X-ray diffraction (XRD) patterns were recorded at room temperature using a Seifert-XRD 3000 diffractometer with a $\text{Cu K}\alpha$ radiation ($\lambda = 0.15418 \text{ nm}$) in the 2θ range of $2\text{--}20^\circ$ at a scanning rate of $0.02^\circ \text{ min}^{-1}$. Surface area, pore volume and pore size distributions were obtained from N_2 adsorption–desorption isotherms determined at 77 K using a Micromeritics ASAP 2010 apparatus and the conventional BET and BJH methods, and the H–J standard curve. Thermal analysis for acidity evaluation was effected in a Perkin Elmer TGS2 thermobalance equipped with a temperature controller system 7/4 and a data station DS3700. Measurements were taken at room temperature by ammonia adsorption using a method described previously (Salerno et al., 2001).

Temperature-programmed reduction (TPR) experiments were performed in a conventional apparatus equipped with a thermal conductivity detector. The samples (200 mg) were loaded in the TPR reactor and pre-treated at 373 K in air for 2 h. After this pre-treatment, the sample were cooled to room temperature and then the air flow was replaced by a reductive mixture of 15 vol.% H_2 in N_2 ($25 \text{ cm}^3 \text{ min}^{-1}$) and the temperature increased at a heating rate of 10 K min^{-1} up to 1273 K.

Raman spectra were recorded with a Renishaw System 1000 spectrometer equipped with a cooled CCD detector (200 K) and a holographic Notch filter that removes the elastic scattering. The samples were excited with a 514-nm Ar line in an in situ cell (Likan TS-1500), which allows temperature treatments under flowing gases. The spectra acquisition consisted of five accumulation of 60 s each. To avoid fluorescence, samples were pre-treated at 673 K for 2 h.

X-ray photoelectron spectra (XPS) of both calcined and sulfided catalysts were obtained with a Fison Escalab 200R photoelectron spectrometer equipped with a hemispherical electron analyser and a $\text{Mg K}\alpha$ source (1253.6 eV) and operating at 120 W. Powder samples were pressed into small copper supports and then mounted on a support rod placed in the pre-treatment chamber. The intensity of the peaks was estimated by calculating the integral of each peak after smoothing and subtraction of the S-shaped background and fitting the experimental curve to a combination of Gaussian and Lorentzian functions. The surface atomic ratios were computed from the intensity ratios normalised by atomic sensitivity factors. All spectra were referenced to the binding energy (BE) of the C1s peak from carbon contamination of the samples at 284.9 eV. An estimated error of $\pm 0.1 \text{ eV}$ can be assumed for all measurements. Sulfidation of the catalysts was carried out in a glass reactor at atmospheric pressure with a 10 vol.% $\text{H}_2\text{S}/\text{H}_2$ flow at 623 K for 4 h. After sulfidation, the samples were cooled to room temperature in flowing He and then stored under *n*-heptane to avoid contact with air.

2.3. Catalytic activity measurements

The activity of the catalysts for gas oil HDS and pyridine HDN was simultaneously measured in a high-pressure, fixed-bed flow micro-reactor under standard conditions: H_2 pressure 3 MPa; LHSV 90 h^{-1} ; H_2/liquid ratio of 6.67, and reaction temperature 648 K. The feedstock was a gas oil containing 1.87 wt.% of S enriched with 1000 ppm of N in pyridine form. Samples of 200 mg of catalyst (particle size 0.14–0.25 mm), diluted with inert particles of SiC in a volume ratio of 1:5, were sulfided in situ with a 7

vol.% CS₂/gas oil mixture at 2 MPa and 623 K for 4 h. The liquid products were collected from a gas–liquid separator every 30 min and analysed for S and N contents using an Antek sulfur/nitrogen analyser. From fractional conversion, the HDS activity of the catalysts was calculated in terms of pseudo-second order rate constant per volume of catalyst (Gil Llam-bías and López Agudo, 1978).

3. Results

3.1. X-ray diffraction

Fig. 1 shows the XRD patterns of the support (Loc) and calcined Al-PILC supported Mo catalysts. All catalysts displayed the intense lines at 4.9 and 19.9° corresponding to the support 001 and 100 reflections, respectively, and additional weak reflections at 23.3° and 27.3° ascribable to crystalline MoO₃. In general, this means that molybdenum was poorly dispersed in all catalysts. The intensity of the MoO₃ signals increased slightly with decreasing impregnation pH.

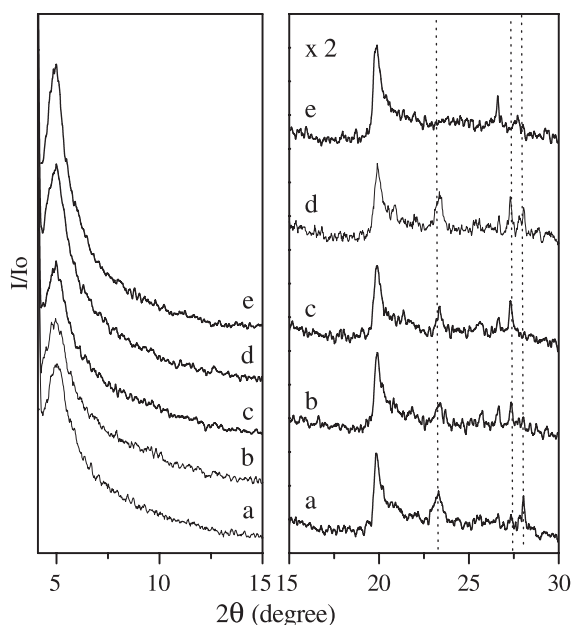


Fig. 1. X-ray diffraction patterns of calcined Mo(x)/Loc catalysts: (a) Mo(10)/Loc; (b) Mo(8.5)/Loc; (c) Mo(6.5)/Loc; (d) Mo(4)/Loc; (e) Loc.

This is in agreement with the findings for alumina- and silica-supported Mo catalysts that at low pH bulk MoO₃ formation is favoured (Kasztelan et al., 1986; López Cordero et al., 1991). In Mo(4)/Loc and Mo(10)/Loc catalysts, a weak peak appeared at 28.0°, which could be assigned to K₂MoO₄ formed with K⁺ cations from the clay.

3.2. Textural analysis

The data of BET surface areas and pore volumes in Table 1 indicate that about a third of the specific surface area and corresponding pore volume of the support was lost through Mo impregnation, denoting a plugging of the pores with Mo species. The reduction of porosity occurred in both the micro and mesopores, increasing from about 20% for Mo(4)/Loc to about 32% for Mo(10)/Loc when the pH of the impregnating solution increased. Since treatment of Loc under the same acidic and basic pH conditions in the absence of Mo did not significantly change the surface area and pore volume of the support (with fluctuations around 2% without a clear trend), the observed reduction in microporosity for catalysts can be attributed to occupation of the pores with Mo species. This pore occupation increased with the impregnation pH because at high pH the Mo species present in solution are predominantly MoO₄²⁻, which can diffuse and penetrate more easily into the Al-PILC pores than the large Mo₇O₂₄⁴⁻ species present at acidic pH.

3.3. Acidity measurements

Data of total acidity, expressed as meq of chemisorbed NH₃ per gram of catalyst, for the calcined catalysts are given in Table 1. With the incorporation of molybdate to the Al-PILC, the concentration of acid sites did not change significantly for Mo(4)/Loc and Mo(8.5)/Loc catalysts and increased slightly for Mo(10)/Loc and Mo(6.5)/Loc catalysts. These slight differences in the concentration of acid sites are probably the net result of several factors such as the change in the pH of impregnation solution, the nature of the molybdate species adsorbed and their amount, and the residual cations or protons present in the sample. No important differences in acid strength among catalysts were observed. For a comparative purpose, the total acidity of the alumina-supported Mo

catalyst used as reference for catalytic activity was 1.1 ± 0.1 meq $\text{NH}_3 \text{ g}^{-1}$.

3.4. TPR results

The TPR profiles of calcined $\text{Mo}(x)/\text{Loc}$ catalysts are shown in Fig. 2. The profiles, quite similar to others reported previously for alumina- and silica-supported Mo catalysts (López Cordero et al., 1991; Regalbuto and Ha, 1994; López Cordero and López Agudo, 2000), showed generally two main reduction peaks with maxima at around 780 and 1015 K. However, there are some differences among the catalysts, particularly in the amount of consumed hydrogen, in the position of the reduction peak maximum (T_{max}) and in the presence of additional shoulders, which indicate differences in the distribution of the supported oxo-molybdenum species. In the studies on the reducibility of supported Mo catalysts (López Cordero et al., 1991; Regalbuto and Ha, 1994; López Cordero and López Agudo, 2000), the lowest-temperature peak has

generally been associated to the $\text{Mo}^{6+} \rightarrow \text{Mo}^{4+}$ reduction step of dispersed polymolybdate-like species, the highest-temperature peak has been attributed to a further $\text{Mo}^{4+} \rightarrow \text{Mo}^0$ reduction plus the reduction of tetrahedral-coordinated molybdate interacting more strongly with the support, and the appearance of an intermediate peak at 840 K to the reduction of bulk MoO_3 . Based on the literature, the broad peak around 780 K observed in $\text{Mo}(10)/\text{Loc}$ can be attributed to the presence of a considerable proportion of polymeric Mo species. However, its broadness and asymmetry towards higher reduction temperature suggests that a small amount of Mo is probably present as dispersed bulk MoO_3 -like species. In contrast, in the profile of $\text{Mo}(4)/\text{Loc}$, the lowest-temperature peak corresponding to polymeric Mo appeared as a small shoulder, while the peak near 828 K is dominant. That means that in $\text{Mo}(4)/\text{Loc}$, the fraction of polymeric Mo is smaller and bulk MoO_3 is more abundant than in $\text{Mo}(10)/\text{Loc}$ and $\text{Mo}(6.5)/\text{Loc}$. In the two later catalysts, most of Mo is as polymeric Mo species. In the case of $\text{Mo}(8.5)/\text{Loc}$, the TPR profile showed basically a single well-defined peak in each temperature region, which according to their positions at about 790 and 1025 K could be, at first, assigned to reduction of polymeric Mo species. However, given the general features of the low-temperature peak, it can be also attributed to the presence of small discrete particles of bulk MoO_3 , which on silica reduces at nearly the same rate than the polymeric Mo species (López Cordero et al., 1991; Regalbuto and Ha, 1994). The small peaks at temperatures near 1105 and 1130 K observed in $\text{Mo}(6.5)/\text{Loc}$ and $\text{Mo}(4)/\text{Loc}$, respectively, can be assigned to isolate molybdate species formed with residual cations of the support.

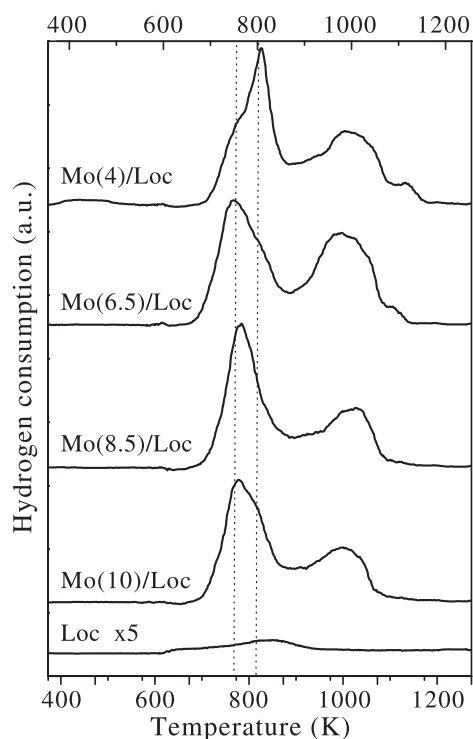


Fig. 2. TPR of calcined $\text{Mo}(x)/\text{Loc}$ catalysts.

Results of the degree of Mo reduction (α), expressed as the ratio of the actual H_2 consumption to the theoretical one (assuming all Mo being as MoO_3 is reduced to Mo^0) are given in Table 2. In general, α was quite low for all samples, specially for $\text{Mo}(10)/\text{Loc}$, suggesting that a substantial part of the oxide Mo species is probably well dispersed and strongly attached to the support (Thomas et al., 1983; López Cordero et al., 1991; Regalbuto and Ha, 1994; López Cordero and López Agudo, 2000), and/or that there are some isolated MoO_4^{2-} species hardly reducible even at high temperatures (>1300 K) in these catalysts. The highest reduction degree found

Table 2
TPR results of calcined Mo(x)/Loc catalysts

Catalyst	TPR peak maximum		Reduction degree, α
	Low region (K)	High region (K)	
Mo(10)/Loc	780, 828 (s)	1015	0.54
Mo(8.5)/Loc	783	1025	0.74
Mo(6.5)/Loc	770, 830 (sh)	1000, 1105 (s)	0.65
Mo(4)/Loc	780 (sh), 828	1000, 1133 (s)	0.67

sh: shoulder; s: small peak.

for Mo(8.5)/Loc ($\alpha=0.74$) is consistent with the presence of well-dispersed MoO₃ micro-crystallites weakly bonded to the support.

3.5. Raman results

In Fig. 3, the Raman spectra of Mo(x)/Loc catalysts pre-treated at 773 K are shown. The spectrum of Mo(4)/Loc could not be measured due to fluorescence problems. Irrespective of the pH used in the impregnation, all catalysts presented two more or less devel-

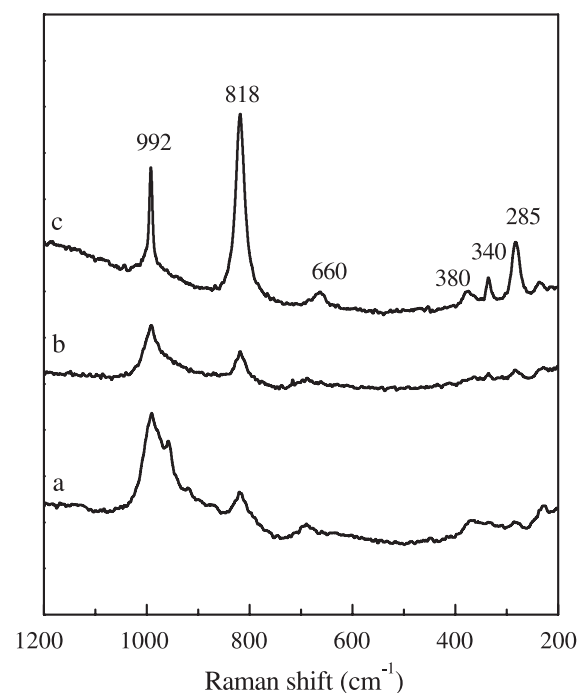


Fig. 3. Raman spectra of calcined catalysts: (a) Mo(10)/Loc; (b) Mo(8.5)/Loc; (c) Mo(6.5)/Loc.

oped peaks at 992 and 818 cm⁻¹ characteristics of crystalline MoO₃, which is consistent with the XRD results. Furthermore, the Mo(6.5)/Loc catalyst exhibited several less intense peaks at 660, 340 and 285 cm⁻¹ which confirm the presence of crystalline MoO₃ (Vuurman and Wachs, 1992; Marchi et al., 1997; Mestl and Srinivasan, 1998) as main component. In contrast, the Mo(10)/Loc catalyst displayed a less developed spectrum with weak peaks at about 960, 870 and 230 cm⁻¹ ascribable to aggregates of polymeric Mo, accompanied probably by some molybdates of the X₂Mo₂O₇ type. Similar general features but with peaks less developed in the spectrum of Mo(8.5)/Loc indicates the presence of micro-crystallites of MoO₃, confirming the above TPR results.

3.6. XPS results

The catalysts in both calcined and sulfided state were studied by XPS. The binding energies (BE) of Si 2p and Mo 3d_{5/2} are summarised in Table 3. The BE of Si 2p (102.6 ± 0.1 eV) was practically unchanged irrespective of the impregnation conditions and the calcined or sulfided state of the catalysts. The Mo 3d spectra for calcined samples consisted of a single Mo 3d doublet with a Mo 3d_{5/2} BE of 232.7 ± 0.1 eV corresponding to oxidic Mo(VI) species. The position of the Mo 3d_{5/2} peak was not significantly altered by the pH of the impregnation solution, indicating no significant differences in the interaction of oxide Mo species and the support among the catalysts. For sulfided catalysts, the Mo 3d spectra were fitted into

Table 3
XPS binding energies (eV) and Mo/Si atomic ratios for calcined and sulfided Mo(x)/Loc catalysts

Catalyst	Si 2p (eV)	Mo 3d _{5/2}		Sulfidation degree (%)	Mo/Si atomic ratio	
		Calc. (eV)	Sulf. (eV)		Calc.	Sulf.
Mo(10)/Loc	102.6	232.7	228.8	74	0.12	0.12
			231.9			
Mo(8.5)/Loc	102.6	232.6	228.7	70	0.10	0.10
			231.5			
Mo(6.5)/Loc	102.5	232.6	228.6	78	0.08	0.13
			231.8			
Mo(4)/Loc	102.7	232.7	228.8	78	0.11	0.15
			231.8			

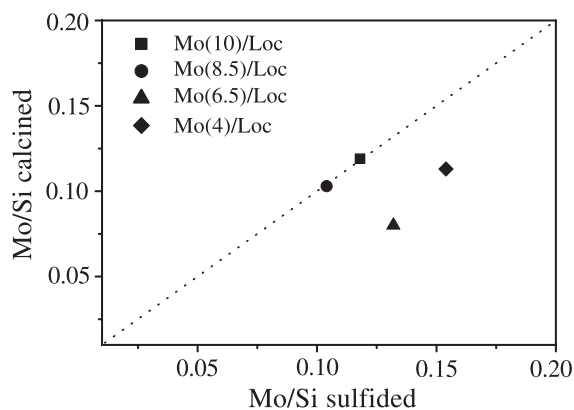


Fig. 4. Comparison of the Mo/Si XPS atomic ratio of oxidic and sulfided Mo(x)/Loc catalysts.

two sets of doublets with the main Mo $3d_{5/2}$ at 228.7 ± 0.1 and $231.9\text{--}231.5$ eV, which can be assigned to Mo(IV) in sulfided state (MoS_2) and to Mo(V) in oxidized and/or oxysulfided state, respectively (Okamoto et al., 1989; Weber et al., 1995). Therefore, it is evident that a significant part of Mo species was not completely sulfided under the sulfidation conditions used. In Table 3 are listed the degree of Mo sulfidation calculated by dividing the area corresponding to Mo(IV) by total Mo. It is observed that the sulfidation of Mo increased slightly for acidic prepared catalysts.

The estimated Mo/Si surface atomic ratios are also given in Table 3. For both calcined and sulfided samples, the variation of the Mo/Si ratio as a function of the impregnation pH was very small and did not follow a clear trend. The measured Mo/Si ratios were in most of cases slightly higher than the theoretical bulk Mo/Si ratio (0.08), indicating certain enrichment and probably aggregates of Mo on the external surface of the support. The effect of the sulfidation treatment on the distribution of Mo species for the different catalysts can be estimated by plotting the Mo/Si ratios for calcined samples versus the same ratio for sulfided samples (Fig. 4). It is evident that the Mo/Si ratio significantly changed after sulfidation for the catalysts prepared at acidic pH and remained virtually unchanged for the catalysts prepared at basic pH. The deviation from linearity observed for acidic catalyst preparations indicates that sulfidation increased the aggregation of the Mo species, probably due to a weaker interaction of the Mo species with the support and the presence of crystalline MoO_3 in the calcined catalysts.

3.7. Catalytic activity

A comparison of the steady state activity for gas oil HDS of the Mo(x)/Loc catalysts, the support alone and a sample of Mo supported on the starting clay is presented in Fig. 5. The support Loc and the Mo/

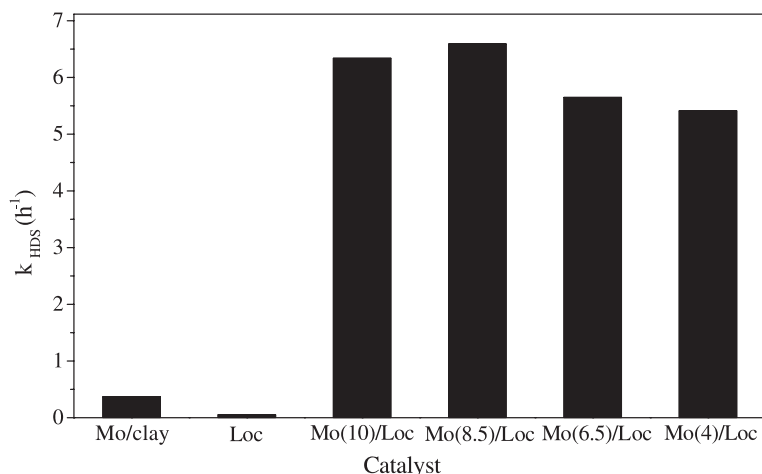


Fig. 5. Comparison of the catalytic activity for the support Loc, Mo/clay and Mo(x)/Loc catalysts in the HDS of gas oil at 643 K.

starting clay samples were hardly active for gas oil HDS. The Mo(10)/Loc and Mo(8.5)/Loc catalysts prepared at basic pH had slightly higher HDS activity than the Mo(6.5)/Loc and Mo(4)/Loc ones prepared at acidic pH. None of catalysts showed appreciable activity for pyridine HDN after 9-h reaction time.

4. Discussion

In the preparation of Mo-supported catalysts by impregnation with aqueous solution of AHM, it is well established that the pH of the impregnating solution regulates the proportion of the type of molybdates present in solution (monomeric MoO_4^{2-} at $\text{pH} \geq 7$ –8 and polymeric $\text{Mo}_7\text{O}_{24}^{4-}$ at pH below ~ 5.5) and also the molybdate adsorption on the surface of the support according to its isoelectric point (IEP) (Hall, 1982). Therefore, in the case of Al-PILC (IEP=3.2) its behaviour on molybdate adsorption is expected to be similar to that of silica (IEP=3.0, López Cordero et al., 1991). However, the presence of free alumina (from some excess of hydroxyl-aluminium polycations used in pillaring) on the PILC surface (Salerno et al., 2001), or coordinatively unsaturated Al at the edges of the layers may give rise to specific spots in which the IEP of alumina (IEP=8.9, López Cordero et al., 1991) dominates and the molybdate adsorption is different to that on the silica part.

On this basis, in the case of Mo(10)/Loc, as the pH of the impregnation solution was much higher than the IEP of the Al-PILC support, the Al-PILC was negatively charged and no adsorption of the predominant MoO_4^{2-} species in solution took place. Under such unfavourable conditions for anion adsorption on the clay surface (the interaction between MoO_4^{2-} and Al-PILC surface is weak), most of the MoO_4^{2-} remained for a long time in solution, allowing some MoO_4^{2-} species to move into the interlayer space of the Al-PILC. As a consequence, after drying some Mo deposited in the form of monomeric MoO_4^{2-} into the interlayer space of the Al-PILC. The large decrease in micropore volume of the Mo(10)/Loc with respect to that of the support confirms the diffusion and location of some molybdates inside the Al-PILC porous system. Consistently, the low Mo reduction degree for Mo(10)/Loc ($\alpha=0.54$) indicates the presence of strongly bonded molybdate species, probably to the

alumina pillars, or irreducible metal molybdates (as shown by XRD), in the interlayer space of the clay. However, as in general the molybdate adsorption was not favoured, a substantial part of molybdate species was deposited on the surface of the clay in the form of polymeric Mo species, as TPR and Raman suggested.

In contrast, in the case of Mo(4)/Loc, as the impregnation pH was quite close to the IEP of the Al-PILC support and the surface was positively charged, the adsorption is favoured and molybdate (in this case, predominantly presents in solution as $\text{Mo}_7\text{O}_{24}^{4-}$ species) would be strongly adsorbed. However, this adsorption will occur mostly on the external surface of the Al-PILC since the large $\text{Mo}_7\text{O}_{24}^{4-}$ species have less chance to diffuse into the Al-PILC layers and to occupy such internal positions, reflected in the relatively higher pore volume value exhibited for this catalyst (Table 1). In the drying step, these $\text{Mo}_7\text{O}_{24}^{4-}$ species, adsorbed or deposited on the external surface of the Al-PILC, will lead to the formation of polymeric Mo and aggregates of bulk MoO_3 . Indeed, the TPR profile of Mo(4)/Loc (Fig. 2) clearly shows the formation of a relatively low amount of polymeric Mo and abundant amount of bulk MoO_3 in this catalyst, as the XRD also indicated.

At impregnation pH 6.5, since both MoO_4^{2-} and $\text{Mo}_7\text{O}_{24}^{4-}$ species are present in solution and only the surface of the alumina component is protonated, the adsorption behaviour is intermediate to that described for the catalysts prepared to pH 10 and 4, but closer to the later one. Therefore, in Mo(6.5)/Loc was found: a large amount of polymeric Mo (TPR profile), a detectable fraction of bulk MoO_3 (confirmed by Raman) and no significant amount of molybdates inside the interlayer space (N_2 adsorption).

In the case of impregnation at pH 8.5, catalyst Mo(8.5)/Loc, the situation is something different because the impregnation medium was a dilute H_2O_2 solution. In this medium, the stability and solubility of AHM solutions is markedly increased due to the formation of their peroxy species (Tsigdinos et al., 1981). As a consequence, the peroxy AHM species can diffuse and distribute more easily and homogeneously in the pores and particles of the Al-PILC, which will deposit in small aggregated Mo species or micro-crystallites of a MoO_3 -like phase relatively and highly dispersed upon drying and calcination. The XRD and Raman results showed

the formation of these MoO₃ microcrystallites, which is consistent with the highest Mo reduction degree of this catalyst and the position of the TPR low-temperature peak. In this catalyst, like in Mo(10)/Loc, a small part of Mo is most likely located in the interlayer space of the Al-PILC since the micropore volume decreased significantly with the incorporation of Mo.

From the above discussion, we can conclude that the pH of impregnation solution induces notable differences in the distribution and dispersion of the Mo species in the oxidic state of the catalysts. These differences determine the behaviour of the catalysts under sulfidation since bulk MoO₃ apparently sulfides more easily than polymolybdate species, and likely undergoes further aggregation along the sulfidation process when a weak metal-support interaction is involved, leading then to a low dispersion of the active MoS₂ phase.

The results of HDS activity shown in Fig. 5 can, therefore, be related to the changes in dispersion and distribution of the Mo phase in the PILC above discussed. The slightly higher HDS activities of Mo(8.5)/Loc and Mo(10)/Loc may be attributed to two characteristics of these catalysts: (i) a better dispersion of the Mo active phase on the Al-PILC surface, in both the oxide and sulfided state; and (ii) the incorporation of a part of the Mo active phase within the porous of the support. The Mo oxide species located inside the pores of the Al-PILC will provide, with respect to those outside the pores, not only smaller MoS₂ particles sterically limited by the pores, but also the possibility of a synergetic effect between the acidic sites and the active sulfided Mo phase similar to that observed in metal sulfides supported on zeolites (Welters et al., 1994). The slightly lower HDS activities of Mo(6.5)/Loc and Mo(4)/Loc samples reflect the lower dispersion of the Mo species in these catalysts, which in the oxide state have relatively large amounts of Mo in form of bulk MoO₃ on the external surface of the Al-PILC. Therefore, based on the data obtained in this study, the dispersion and location of Mo species in the Al-PILC rather than the degree of sulfidation of Mo is the factor determining the HDS activity of the present Mo(x)/Al-PILC catalysts.

In order to see the behaviour of Al-PILC as support of Mo catalysts, it is interesting to compare the present

activity results with those reported in the literature for γ -Al₂O₃ supported catalysts. The HDS activities per Mo atom of the Al-PILC supported Mo catalysts were slightly higher or about the same than their γ -Al₂O₃-supported counterparts (López Cordero et al., 1989; López Cordero and López Agudo, 2000). The lower acidity for the alumina-supported Mo catalysts with respect to the Al-PILC supported Mo catalyst supports the above suggestion that the acid sites of the Al-PILC may induce a synergetic effect in HDS activity. Therefore, it appears that Al-PILCs result promising as support of Mo hydrotreating catalysts and invite for further research on promoted Ni(Co)Mo/Al-PILC systems.

5. Conclusions

Molybdenum oxide supported on an Al-pillared montmorillonite synthesised by the “slurry” method is a thermal stable material with high specific area, which upon sulfidation has a high catalytic activity for gas oil HDS. Consequently, Mo supported on Al-pillared clays seem to be promising hydrotreating catalysts.

Concerning Mo impregnation, the Al-PILC surface behaves rather like silica than alumina. The nature and distribution of Mo species throughout the Al-pillared clay and, hence, the catalytic activity of these materials, is slightly dependent on the pH of the impregnation solution in conjunction with the porous system of the Al-pillared clay support. Increasing the impregnation pH leads to a better molybdenum dispersion, more incorporation of molybdate species into the interlayer space of the clay, and after sulfidation less segregation of bulk MoS₂ on the mesopores and the external surface of the Al-PILC, and hence to a higher HDS catalyst activity. Impregnation at pH 8.5 (in a H₂O₂ solution) gives rise to a higher dispersion of Mo on the Al-PILC surface than impregnation at pH 10 (ammonia solution), leading to a slightly higher HDS activity for the former catalyst preparation.

Acknowledgements

We are grateful to the DGICYT, Ministry of Education and Science, Spain, project PB96-0913 for financial support, and to the Agencia Española de

Cooperación Internacional for the award of a doctoral fellowship to P. Salerno. Also, the authors thank Dr. J.L.G. Fierro for XPS measurements and Dr. M.A. Bañares for Raman measurements.

References

- Burch, R., 1987. Introduction. *Catal. Today* 2, 185–186.
- Burch, R., Warburton, C.I., 1987. Pillared clays as demetallisation catalysts. *Appl. Catal.* 33, 395–404.
- Figueras, F., 1988. Pillared clays as catalysts. *Catal. Rev., Sci. Eng.* 30, 457–499.
- Gil, A., Gandía, L.M., Vicente, M.A., 2000. Synthesis and catalytic application of pillared clays. *Catal. Rev., Sci. Eng.* 42, 145–212.
- Gil Llambías, F.J., López Agudo, A., 1978. Hidrodesulfuración catalítica de gas-oil. I. Selección de las condiciones de operación para la evaluación de catalizadores. *An. Quim.* S1, 1–6.
- Hall, W.K., 1982. The genesis and properties of molybdena-alumina and related catalyst systems. In: Barry, H.F., Mitchell, P.C.H. (Eds.), *Proceedings of the Climax Fourth International Conference on the Chemistry and Uses of Molybdenum*. Climax Molybdenum, Ann Arbor, MI, pp. 224–233.
- Kasztelan, S., Payen, E., Toulhoat, H., Grimblot, J., Bonnelle, J.P., 1986. Industrial MoO₃-promoter oxide- γ -Al₂O₃ hydrotreating catalysts: genesis and architecture description. *Polyhedron* 5, 157–167.
- Kloproge, J.T., Welters, W.J.J., Booy, E., de Beer, V.H.J., van Santen, R.A., Geus, J.W., Jansen, J.B.H., 1993. Catalytic activity of nickel sulfide catalysts supported on Al-pillared montmorillonite for thiophene hydrodesulfurization. *Appl. Catal.*, A 97, 77–85.
- Lambert, J.F., Poncelet, G., 1997. Acidity in pillared clays: origin and catalytic manifestations. *Top. Catal.* 4, 43–56.
- López Cordero, R., López Agudo, A., 2000. Effect of water extraction on surface properties of Mo/Al₂O₃ and NiMo/Al₂O₃ hydrotreating catalysts. *Appl. Catal.*, A 202, 23–35.
- López Cordero, R., Esquivel, N., Lázaro, J., Fierro, J.L.G., López Agudo, A., 1989. Effect of phosphorous on molybdenum-based hydrotreating catalysts. I. Characterization of the oxide state of P-Mo/Al₂O₃ systems. *Appl. Catal.*, A 48, 341–352.
- López Cordero, R., Gil Llambías, F.J., López Agudo, A., 1991. Temperature-programmed reduction and zeta potential studies of the structure of MoO₃/Al₂O₃ and MoO₃/SiO₂ catalysts. Effect of the impregnation pH and molybdenum loading. *Appl. Catal.*, A 74, 125–136.
- Louloudi, A., Papayannakos, N., 2000. Hydrogenation of benzene on Ni/Al-pillared montmorillonite catalysts. *Appl. Catal.*, A 204, 167–176.
- Lur'e, M.A., Kurets, I.Z., Kushnarev, D.F., Malyuchenko, A.A., Schmidt, F.K., 2000. Formation, physicochemical, and catalytic properties of the Mo containing hydrotreatment catalysts on various supports: IV. The activity of the catalysts for the hydrotreatment of black oil. *Kinet. Katal.* 41, 57–60.
- Marchi, A.J., Ledo, E.J., Requejo, F.G., Rentería, M., Irusta, S., Lombardo, E.A., Miró, E.E., 1997. Laser Raman Spectroscopy (LRS) and time differential perturbed angular correlation (TDPAC) study of surface species on Mo/SiO₂ and Mo, Na/SiO₂. Their role in the partial oxidation of methane. *Catal. Lett.* 48, 47–54.
- Mestl, G., Srinivasan, T.K.K., 1998. Raman spectroscopy of monolayer-type catalysts: supported molybdenum oxides. *Catal. Rev., Sci. Eng.* 40, 451–570.
- Monnier, J., Charland, J.P., Brown, J.R., Wilson, M.F., 1993. Hydrotreating gas oils from synthetic crude with mixed pillared clay-alumina supported catalysts. *Stud. Surf. Sci. Catal.* 75, 1943–1946.
- Moreno, S., Gutierrez, E., Alvarez, A., Papayannakos, N.G., Poncelet, G., 1997. Al-pillared clays, from lab syntheses to pilot scale production. Characterization and catalytic properties. *Appl. Catal.*, A 165, 103–114.
- Okamoto, Y., Maezawa, A., Imanaka, T., 1989. Active sites of molybdenum sulfide catalysts supported on Al₂O₃ and TiO₂ for hydrodesulfurization and hydrogenation. *J. Catal.* 120, 29–45.
- Pacheco, J.G., de los Reyes, J.A., Fuentes, G.A., 1998. Efecto de la concentración de fase activa en catalizadores MoS₂/arcilla pillareda con Al–Ga en la HDS del tiofeno. In: Centeno, A., Giraldo, S.A., Páez Moro, E.A. (Eds.), *Actas del XVI Simposio Iberoamericano de Catálisis*. Centro de Investigaciones en Catálisis, UIS, Bucaramanga, Colombia, pp. 55–60.
- Pinnavaia, T.J., 1983. Intercalated clay catalysts. *Science* 220 (4595), 365–372.
- Ramos-Galvan, C.E., Sandoval-Robles, G., Castillo-Mares, A., Dominguez, J.M., 1997. Comparison of catalytic properties of NiMo/Al₂O₃ with NiMo supported on Al-, Ti-pillared clays in HDS of residual oils. *Appl. Catal.*, A 150, 37–52.
- Regalbutto, J.R., Ha, J.W., 1994. A corrected procedure and consistent interpretation for temperature programmed reduction of supported MoO₃. *Catal. Lett.* 29, 189–207.
- Salerno, P., Asenjo, M.B., Mendioroz, S., 2001. Influence of preparation method on thermal stability and acidity of Al-PILCs. *Thermochim. Acta* 379, 101–109.
- Sanchez, A., Montes, M., 1998. Influence of the preparation parameters (particle size and aluminium concentration) on the textural properties of Al-pillared clays for a scale-up process. *Microporous Mesoporous Mater.* 21, 117–125.
- Storaro, L., Lenarda, M., Rinaldi, A., 1996. Preparation of hydroxy Al/Fe pillared bentonites from concentrated clay suspensions. *Microporous Mesoporous Mater.* 6, 55–63.
- Sychev, M., de Beer, V.H.J., Kodentsov, A., van Oers, E.M., van Santen, R.A., 1997. Chromia- and chromium sulfide-pillared clays, preparation, characterization, and catalytic activity for thiophene hydrodesulfurization. *J. Catal.* 168, 245–254.
- Thomas, R., van Oers, E.M., de Beer, V.H.J., Moulijn, J.A., 1983. Characterization of silica-supported molybdenum oxide and tungsten oxide. Reducibility of the oxidic state versus hydrodesulfurization activity of the sulfided state. *J. Catal.* 84, 275–287.
- Topsoe, H., Clausen, B.S., Massoth, F.E., 1996. Hydrotreating catalysts. In: Anderson, J.R., Boudart, M. (Eds.), *Catalysis Science and Technology*, vol. 11. Springer, Berlin, pp. 65–95.
- Tsigdinos, G.A., Chen, H.Y., Streusand, B.J., 1981. Molybdate solutions for catalyst preparation. Stability, adsorption proper-

- ties, and characterization. *Ind. Eng. Chem. Prod. Res. Dev.* 20, 619–623.
- Vaccari, A., 1999. Clays and catalysis, a promising future. *Appl. Clay Sci.* 14, 61–198.
- Vuurman, M.A., Wachs, I.E., 1992. In situ Raman spectroscopy of alumina-supported metal oxide catalysts. *J. Phys. Chem.* 96, 5008–5016.
- Weber, Th., Muijsers, J.C., Niemanntsverdriet, J.W., 1995. The structure of amorphous MoS₃. *J. Phys. Chem.* 99, 9194–9200.
- Welters, W.J.J., de Beer, V.H.J., van Santen, R.A., 1994. Influence of zeolite acidity on thiophene hydrodesulfurization activity. *Appl. Catal., A* 119, 253–269.